

## Amugulang virus, a novel hantavirus harboured by small rodents in Hulunbuir, China

Xiaohu Han<sup>a\*</sup>, Lianhong Zhang<sup>a\*</sup>, Mingxuan Zhang<sup>b\*</sup>, Qing Xin<sup>a</sup>, Yongxiang Zhao<sup>c</sup>, Ya Wen<sup>c</sup>, Hua Deng<sup>b</sup>, Jinguo Zhu<sup>b</sup>, Qin Dai<sup>b</sup>, Mei Han<sup>a</sup>, Tianyu Yang<sup>a</sup>, Saiji Lahu<sup>d</sup>, Feng Jiang<sup>a</sup> and Zeliang Chen<sup>a</sup>

<sup>a</sup>Key Laboratory of Livestock Infectious Diseases, Ministry of Education, and Key Laboratory of Ruminant Infectious Disease Prevention and Control (East), Ministry of Agriculture and Rural Affairs, College of Animal Science and Veterinary Medicine, Shenyang Agricultural University, Shenyang, People's Republic of China; <sup>b</sup>Manzhouli International Travel Health Care Center, Manzhouli, Inner Mongolia, People's Republic of China; <sup>c</sup>The Sixth People's Hospital of Dandong City, Dandong, Liaoning, People's Republic of China; <sup>d</sup>Tongliao Centers for Disease Control and Prevention, Tongliao, Inner Mongolia, People's Republic of China

### ABSTRACT

The Hulunbuir region, known for its diverse terrain and rich wildlife, is a hotspot for various natural epidemic diseases. Between 2021 and 2023, we collected 885 wild rodent samples from this area, representing three families, seven genera, and eleven species. Metagenomic analysis identified three complete nucleic acid sequences from the S, M, and L segments of the *Hantaviridae* family, which were closely related to the Khabarovsk virus. The nucleotide coding sequences for S, M, and L (1392 nt, 3465 nt, and 6491 nt, respectively) exhibited similarities of 82.34%, 81.68%, and 81.94% to known sequences, respectively, while protein-level analysis indicated higher similarities of 94.92%, 94.41%, and 95.87%, respectively. Phylogenetic analysis placed these sequences within the same clade as the Khabarovsk, Puumala, Muju, Hokkaido, Topografov, and Tatenalense viruses, all of which are known to cause febrile diseases in humans. Immunofluorescence detection of nucleic acid-positive rodent kidney samples using sera from patients with hemorrhagic fever and renal syndrome confirmed the presence of viral particles. Based on these findings, we propose that this virus represents a new member of the *Hantaviridae* family, tentatively named the Amugulang virus, after its primary distribution area.

**ARTICLE HISTORY** Received 25 March 2024; Revised 16 August 2024; Accepted 21 August 2024





**KEYWORDS** Hantavirus; Amugulang virus; Hulunbuir; Amugulang Port; emerging infectious diseases

### Introduction


The rapid expansion of the diversity of *Bunyaviricetes* in recent years, their significant clinical importance, and recent changes in the advanced classification structure of *Bunyaviruses* have prompted continuous adjustments to their classifications. In 2017, the International Committee on the Taxonomy of Viruses (ICTV) officially reclassified *Bunyaviridae* as *Bunyavirales*, elevating the former genus Hantavirus to the family *Hantaviridae*. On April 26, 2024, the ICTV further upgraded *Bunyavirales* to the class *Bunyaviricetes*. *Hantaviridae* is an important branch of the *Bunyaviricetes* and *Elliovirales*. Despite these updates, the terms “hantavirus” and “*orthohantavirus*” are still commonly used to describe members of *Hantaviridae*. Hantaviruses are characterized by segmented, linear,

single-stranded, negative-sense, or ambisense RNA genomes. This family is the largest among the negative-stranded RNA viruses and can infect a wide range of hosts, including vertebrates, invertebrates, and plants, with some species capable of crossing host barriers [1,2]. Only rodent-borne hantaviruses are associated with human disease [3].

As of November 2023, ICTV records indicated 75 identified hantaviruses, with at least 25 known to cause hantavirus pulmonary syndrome (HPS) or hemorrhagic fever with renal syndrome (HFRS). Key pathogenic hantaviruses include the Hantaan virus (HTNV), Seoul virus (SEOV), Dobrava-Belgrade virus, Tula virus, and Puumala virus (PUUV), primarily associated with HFRS. In contrast, the Andes virus, Chocloense orthohantavirus, and Sin Nombre virus

**CONTACT** Feng Jiang  [jf8849@163.com](mailto:jf8849@163.com)  Key Laboratory of Livestock Infectious Diseases, Ministry of Education, and Key Laboratory of Ruminant Infectious Disease Prevention and Control (East), Ministry of Agriculture and Rural Affairs, College of Animal Science and Veterinary Medicine, Shenyang Agricultural University, 120 Dongling Road, 110866, Shenyang, People's Republic of China; Zeliang Chen  [chenzliang5@mail.sysu.edu.cn](mailto:chenzliang5@mail.sysu.edu.cn)  Key Laboratory of Livestock Infectious Diseases, Ministry of Education, and Key Laboratory of Ruminant Infectious Disease Prevention and Control (East), Ministry of Agriculture and Rural Affairs, College of Animal Science and Veterinary Medicine, Shenyang Agricultural University, 120 Dongling Road, 110866, Shenyang, People's Republic of China

\*These authors contributed equally to this work.

 Supplemental data for this article can be accessed online at <https://doi.org/10.1080/22221751.2024.2396893>.

© 2024 The Author(s). Published by Informa UK Limited, trading as Taylor & Francis Group, on behalf of Shanghai Shangyixun Cultural Communication Co., Ltd. This is an Open Access article distributed under the terms of the Creative Commons Attribution-NonCommercial License (<http://creativecommons.org/licenses/by-nc/4.0/>), which permits unrestricted non-commercial use, distribution, and reproduction in any medium, provided the original work is properly cited. The terms on which this article has been published allow the posting of the Accepted Manuscript in a repository by the author(s) or with their consent.

are linked to HPS. Given the overlap in clinical symptoms between HFRS and HPS, some experts have proposed a unified clinical syndrome called “hantavirus fever,” although this terminology has not been universally adopted [4]. Annually, there are an estimated 150,000–200,000 cases of HFRS or HPS worldwide, with fatality rates varying significantly depending on the virus type. For instance, the Andes virus and Sin Nombre virus in the Americas have fatality rates of 30–50%, HTNV and SEOV around 1%, and PUUV in Europe around 0.1–0.4% [5]. Various hantaviruses can asymptotically infect wild animals and livestock, with rodents, shrews, and bats being common natural hosts.

The ongoing discovery of hantaviruses has underscored their considerable threat to public health. Since Professor Ho Wang Lee identified the first hantavirus in South Korea, six members of the *Hantaviridae* have been identified: HTNV (1976), SEOV (1982), Soochong virus (2006), Muju virus (2007), Linjin virus (2009), and Jeju virus (2012), with HTNV, SEOV, and Muju virus being pathogenic to humans [6,7].

PUUV, identified in Finland in 1980, is prevalent in Central, Northern, and Eastern Europe, causing approximately 3,000 cases annually between 2010 and 2020, typically with mild symptoms and less than 1% mortality [8]. The primary host of PUUV is *Myodes rufocanus*. In 2019, a novel PUUV strain was identified in small rodents in northwestern Ukraine [9]. To date, eight PUUV subtypes have been identified in Europe and Russia, with PUUV-like viruses being found in Japan, South Korea, and Jilin Province, China. PUUV does not affect host animal growth or reproduction but can cause mild HFRS in humans [10]. Of the 75 *Hantaviridae* members, 50 have not been confirmed to infect humans [11–15].

Hantaviruses are enveloped, segmented RNA viruses approximately 120–160 nm in diameter, comprising three genome segments: S (1.8 k nt), M (3.7 k nt), and L (6.5 k nt), which encode nucleoproteins, glycoproteins, and polymerase proteins, respectively [16,17]. Classification methods for *Hantaviridae* remain unstandardized, with some researchers suggesting amino acid sequence similarity thresholds for the S and M segments [14,18]. However, the ICTV emphasizes genome differences, host characteristics, and pathogenicity as classification criteria. Scholars advocate for continuous classification updates in line with new viral discoveries and methodologies [2].

In this study, we identified a novel member of the *Hantaviridae* family through metagenomic sequencing, named the Amugulang virus, based on its distribution area. Preliminary investigations of its prevalence in various regions and rodent species were conducted using electron microscopy and genetic evolutionary analyses.

## Materials and methods

### Sample collection and processing

Wild rodents were collected between 2021 and 2023 from various locations in the Hulunbuir border region of Inner Mongolia, including Arihasate Port, Manzhouli City (Shibali Village and Chagan Lake), Ebuduge Port, Heishantou Port, and Aershan Port. The rodents were trapped in cages, morphologically identified, and euthanized under ether anesthesia. The liver, spleen, lungs, and kidneys were aseptically collected and stored in liquid nitrogen. Species identification was performed as previously described [19]. The study was approved by Shenyang Agricultural University (Letter Number: 2021040701).

### Metagenomic sequencing and sequence assembly

Lung and kidney samples from wild rodents were thoroughly ground, and total RNA was extracted and quantified using a Qubit 4. Libraries were constructed and analyzed using a Qubit 4 and Qseq100, and were considered qualified if the RNA concentration was  $>5$  ng/ $\mu$ L with peak segments in the 300–500 bp range. High-throughput sequencing was performed using an MGISEQ-2000 sequencer. Sequencing data were processed using fastp (version 0.23.4) to remove adapters and low-quality sequences, resulting in clean data. HISAT2 (version 2.2.1) was used to align the clean data with the host genome, resulting in Rmhost data. MEGAHIT (v1.2.9) was employed for de novo assembly of Rmhost data to obtain contigs. The contigs were compared to the nucleotide database using BLASTN (2.14.0+), and annotation was based on the taxonomy database of the National Center for Biotechnology Information. BWA (version 0.7.17-r1188) was used to index the assembled contig sequences, and the mapped reads were aligned to these sequences to obtain the assembly results.

### Epidemiological investigation

cDNA was synthesized from 100 mg of lung and kidney tissues using the EasyPure® Simple Viral DNA/RNA Kit and HiScript® III 1st Strand cDNA Synthesis Kit. Nested PCR primers based on the metagenomic sequencing results were used to detect viral nucleic acids in all samples. Quantitative fluorescence PCR (qPCR) primers and probes were designed for detection in inoculated cells and BALB/c and Kunming mice. Primer and probe sequences are listed in Supplementary Table S1. Positive plasmid standards were synthesized using the detailed sequences provided in Attachment 1.

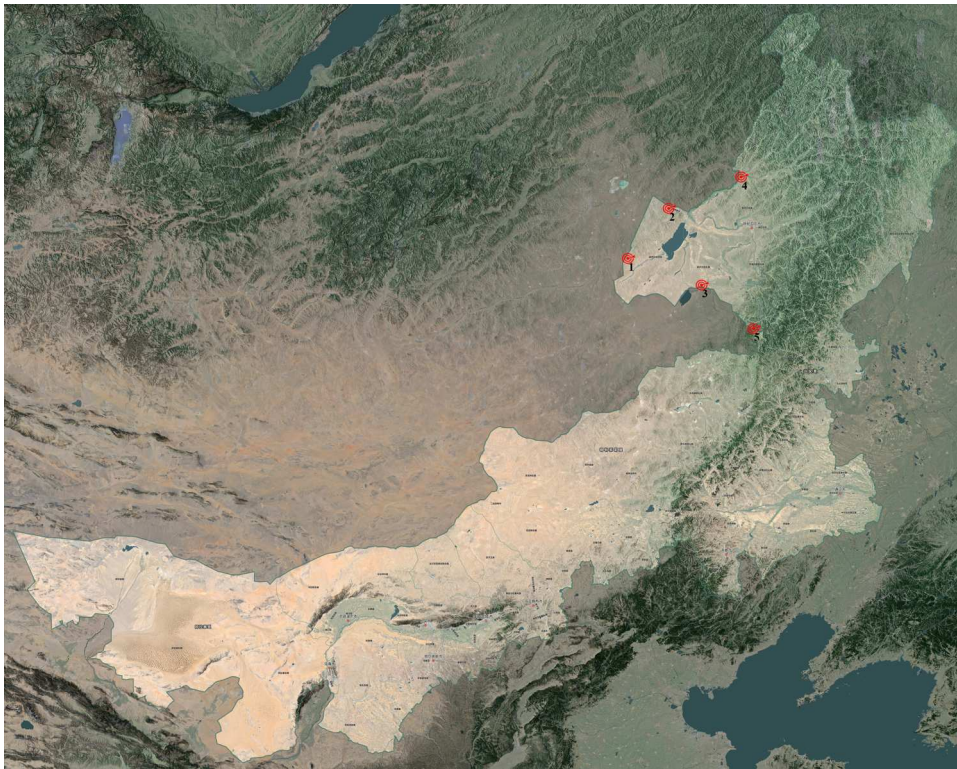


**Figure 1.** Site of sample collection.

### Transmission electron microscopy and indirect immunofluorescence observation

Kidneys from positive wild rodents were sectioned, and viral particles were observed by electron microscopy after negative staining (detailed methods are provided in Attachment 2). Positive sera from clinically diagnosed patients with HFRS (from the Sixth People's Hospital of Dandong City) were used as the primary antibody, and FITC-labeled goat anti-human Fab segment antibody was used as the secondary antibody. Fluorescent staining of frozen sections was performed, and specific fluorescence in the cytoplasm indicated positive staining (detailed methods are presented in Attachment 3).

### Viral isolation

Viral isolation was performed as previously described [20]. Lungs and kidneys from positive rodent samples were ground, suspended in sterile phosphate-buffered saline (PBS), and centrifuged at 1000 ×g to obtain the supernatant, which was filtered through a 0.22 μm filter and stored. Vero and BHK-21 cells were cultured in Dulbecco's modified Eagle's medium supplemented with 10% fetal bovine serum. The cells were washed with PBS, digested with trypsin, centrifuged, mixed with the filtrate, centrifuged again at 1000 ×g for 1 h, and transferred to culture flasks. The supernatant was collected at each passage for nucleic acid extraction and reverse transcription. The filtrate was inoculated into 21-day-old BALB/c and Kunming mice via

the abdominal and nasal cavities. Cell morphology was observed, and nucleic acids were extracted from the mouse lungs and kidneys on days 3, 7, 14, and 21 for viral detection.

### Phylogenetic analyses

The sequences of the latest members of the *Hantaviridae* family were retrieved from the ICTV website. The S, M, and L gene segments and corresponding protein sequences were downloaded and combined with the Amugulang virus nucleic acid sequences to create a FASTA file. Molecular phylogenetic trees were constructed using the neighbor-joining (NJ) method in MEGA11 software.

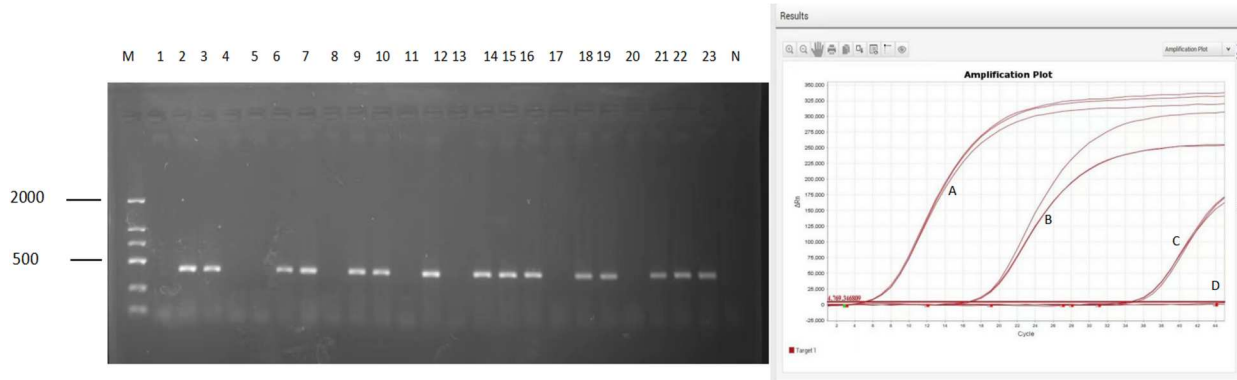
## Results

### Metagenomic identification of Amugulang virus

Between 2021 and 2023, 885 wild rodent samples were collected from the Hulunbuir region, including *Meriones unguiculatus*, *Lasiopodomys brandtii*, *Allactaga sibirica*, *Microtus gregalis*, *Spermophilus dauricus*, *Apodemus agrarius*, *Apodemus peninsulae*, *Phodopus sungorus*, and *Mus musculus*. *L. brandtii* was the dominant species, accounting for 56.3% (498) of the total collected samples. Detailed information on the samples is provided in Attachment 4. Nucleic acid was extracted from pooled samples and subjected to metagenomic sequencing. BLAST analysis of assembled contigs revealed several sequence fragments

**Table 1.** Detection of Amugulang virus in rodent samples from different sampling sites.

Sampling position	East longitude/ north latitude	Landforms	Total number of rodents	Total number of positive rodents	Positive rate (%)
Ebuduge Port	50.2424/120.1909	Grassland	172	25	14.5
Chagan Lake, Manzhouli City	49.58/117.45	Grassland	34	0	0
Heishantou Port	40.234/122.0775	Grassland	75	2	2.7
Arihasate Port	48.5989/115.8815	Grassland	414	17	4.1
Aershan Port	47.1771/119.9431	Forest	152	15	9.9
Shibali Village, Manzhouli City	49.58/117.45	Grassland	38	7	18.4

**Figure 2.** Virus detection results. Left: Amugulang virus detection results

(Note: M: DNA marker-DL2000; N, negative control). Right: qPCR results for inoculated cells, BALB/c mice, and Kunming mice (Note: A: Positive plasmid, B: Positive rodent kidney sample, C: Cell culture supernatant (at day 3), D: Cells washed with PBS (at day 7), and negative control).

highly homologous to those of the family *Hantaviridae*. Positive samples were further confirmed using RT-PCR and Sanger sequencing. The CDS region sequences of the S, M, and L segments, with lengths of 1392, 3465, and 6491 nt respectively, exhibited only 82.34%, 81.68%, and 81.94% similarity to known sequences. Amino acid sequence analysis indicated higher similarities of 94.92%, 94.41%, and 95.87%. These results suggest that these sequences may derive from a new member of the *Hantaviridae* family. Based on virus classification, we tentatively named this virus the Amugulang virus, after its primary distribution area (Figure 1).

### Spatial and host distribution of Amugulang virus

Nucleic acid extracts from all samples were tested by RT-PCR for the presence of the virus sequence. Of the 885 samples tested, 66 were positive, yielding a positivity rate of 7.5% (Table 1 and Figure 2). The distribution of positive samples varied by sampling site, with higher rates at Ebuduge Port (14.5%), Arihasate Port (4.1%), and Aershan Port (9.9%). Notably, Shibali Village in Manzhouli City had the highest positive rate of 18.4%, despite having fewer samples (Table 1). Host species analysis showed that only *L. brandtii* samples were positive for the Amugulang virus, consistent with this species being the most abundant in the region (56.3% of all

samples) (Table 2). Attachment 4 presents the details of the detection results.

### No evidence of vertical transmission of Amugulang virus in pregnant rodents

Four *L. brandtii* samples from Ebuduge Port (three samples) and Arihasate Port (one sample) contained fetuses during dissection. Fetuses (9, 10, 9, and 8, respectively) and their mothers were tested simultaneously. Two maternal samples from Ebuduge Port were nucleic acid positive, but their fetus samples were negative. This result suggests that the virus may not be transmitted vertically from mother to fetus.

### Viral isolation and detection

Given the wide distribution of the virus, we attempted to isolate it by inoculating the positive samples in cells and mice. However, attempts to isolate the virus using Vero and BHK-21 cells, as well as BALB/c and Kunming mice, were unsuccessful. Viral nucleic acids were detected in the culture supernatant of Vero cells on the third and seventh days post-inoculation; however, subsequent tests on washed cells were negative. Continuous cultivation for 21 days yielded negative results. Similarly, lung and kidney samples from inoculated BALB/c and Kunming mice tested negative at 3, 7, 14, and 21 days post-inoculation. The qPCR results are shown in Figure 2.

**Table 2.** Amugulang virus detection in rodent samples.

Rodent species (Latin name)	Family	Genus	Total number of rodents	Total number of positive rodents	Positive rate (%)
<i>Lasiopodomys brandtii</i>	Cricetidae	<i>Microtus</i>	498	66	13.2
<i>Mus musculus</i>	Muridae	<i>Murine</i>	56	0	0
<i>Spermophilus dauricus</i>	Sciuridae	<i>Citellus</i>	11	0	0
<i>Microtus gregalis</i>	Cricetidae	<i>Microtus</i>	108	0	0
<i>Allactaga sibirica</i>	Dipodidae	<i>Allactaga</i>	14	0	0
<i>Apodemus agrarius</i>	Muridae	<i>Apodemus</i>	120	0	0
<i>Meriones unguiculatus</i>	Cricetidae	<i>Meriones</i>	48	0	0
<i>Cricetulus barabensis</i>	Cricetidae	<i>Cricetulus</i>	2	0	0
<i>Rattus norvegicus</i>	Muridae	<i>Rattus</i>	16	0	0
<i>Phodopus sungorus</i>	Cricetidae	<i>Phodopus</i>	4	0	0
<i>Apodemus peninsulae</i>	Muridae	<i>Apodemus</i>	8	0	0

### Virus confirmation by transmission electron microscopy and indirect immunofluorescence

Given the unsuccessful isolation in cell culture and mice, we attempted to observe the virus directly in positive samples. Transmission electron microscopy and immunofluorescence microscopy of kidney samples from infected *L. brandtii* revealed detailed viral morphology. Electron microscopy showed incomplete Amugulang virus particles within Golgi apparatus vesicles, measuring 120–160 nm, as well as mature spherical particles approximately 160 nm in size with visible capsules, characteristic of hantaviruses [16,21–23] (Figure 3). Notably, some viral particles in the cytoplasm and organelles were not fully assembled and measured approximately 120–160 nm.

Since the Amugulang virus belongs to the family *Hantaviridae*, it may be recognized by serum from patients infected with Hantavirus. To confirm this, we collected sera samples from patients with HFRS. RT-PCR positive samples were tested with the serum using indirect immunofluorescence. Immunofluorescence revealed specific green fluorescence in the cytoplasm, indicating the presence of viral particles or proteins, consistent with hantavirus replication patterns (Figure 4). These results suggest cross-

reactivity between Hantavirus and Amugulang virus, indicating that the virus could be recognized by antibodies against Hantavirus (Figure 5).

### Phylogeny of the Amugulang virus

The sequences of the S (Accession: OR767834.1), M (Accession: ON012175.1), and L (Accession: OR767833.1) segments of the Amugulang virus were obtained using metagenomics. Phylogenetic analysis included 75 *Hantaviridae* members from the ICTV directory, with 65 S, 63 M, and 49 L nucleic acid sequences. An NJ tree was constructed using MEGA 11 software (Figure 4), and the results showed that the closest relationship was between the Amugulang and Khabarovsk viruses hosted by *Microtus maximo-wiczii*. Other closely related viruses included Fusong, Hokkaido, Muju, Puumala, Tatenale, and Topografov, all of which belong to the family *Cricetidae*.

Among all the members of the *Hantaviridae* family, the genetic distances between the S, M, and L nucleotide sequences of the Amugulang and Khabarovsk viruses were the lowest, with values of 15.474, 18.196, and 18.647, respectively (Table 3). Genetic distances between the corresponding amino acid sequences were 6.032, 5.975, and 4.231, respectively.

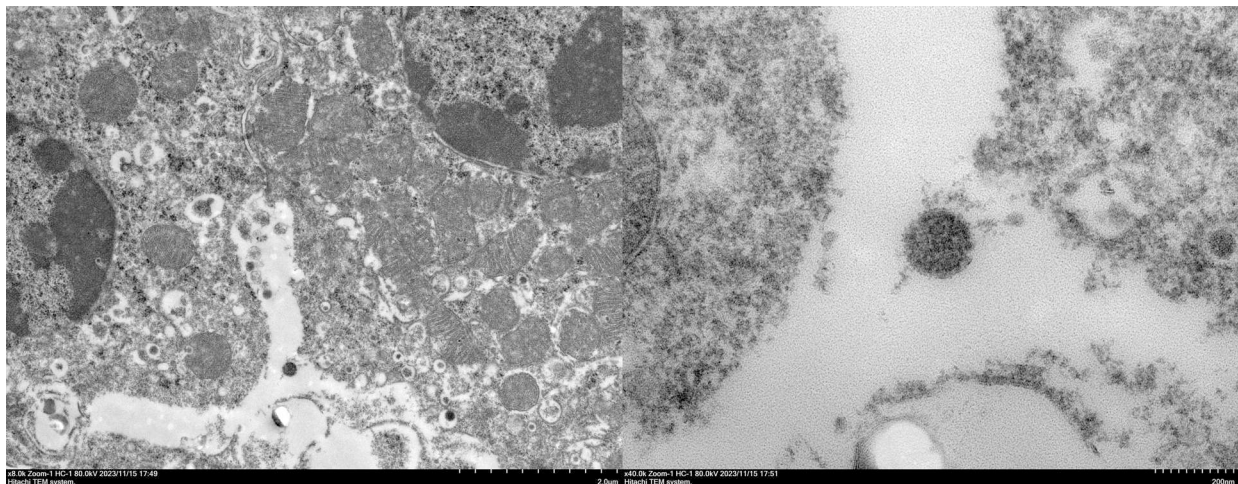


**Figure 3.** Amugulang virus morphology by electron microscopy. Left: Amugulang virus in the Golgi apparatus and vesicles. Scale bar = 200 nm. Right: Free Amugulang virus. Scale bar = 20 nm. The scale bars are located in the lower-right corner of the images.

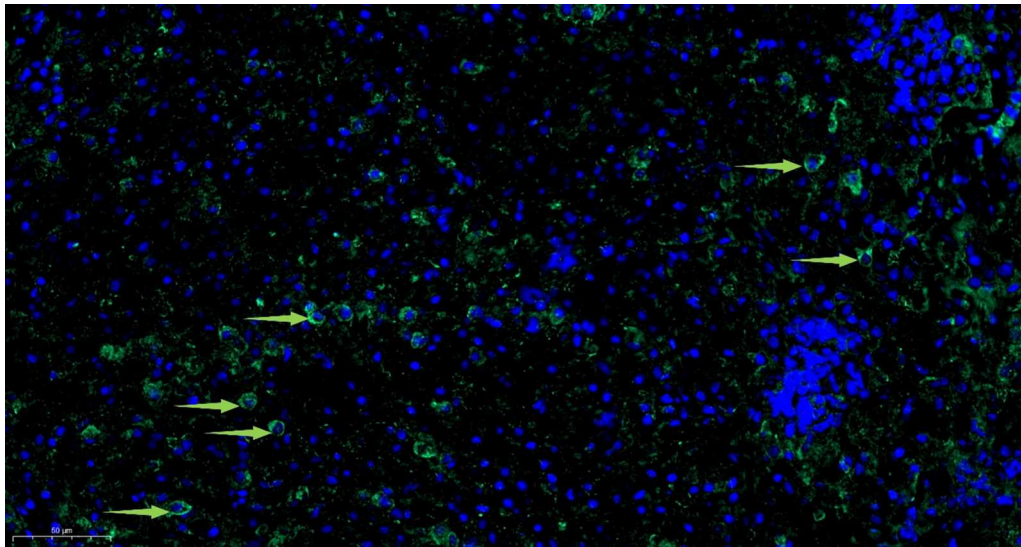


**Figure 4.** Amugulang virus in the kidney by immunofluorescence microscopy. Scale bar = 10 $\mu$ m and is located in the lower-left corner of the image.

According to the literature [2], the nucleotide and amino acid sequences of the S and M segments were concatenated and analyzed, revealing genetic distances of 17.215 and 5.818, respectively. Notably, the hosts of the eight viruses most similar to the Amugulang virus, although different, belong to the *Cricetidae* family.

## Discussion

*Lasiopodomys brandtii* belongs to the family *Cricetidae* and is primarily distributed across China, Mongolia, and Russia, with a concentration in the Hulunbuir region to the west of the Greater Hinggan Mountains. Notably, this species exhibits significant annual population fluctuations, with pronounced peaks occurring approximately every 12 years. *L. brandtii* is a major pest of the temperate grasslands of western Hulunbuir, where it lives in colonies within an extensive burrow system. During population outbreaks, these rodents cause substantial damage to grassland vegetation, contributing to land degradation, desertification, and exacerbating springtime dust storms.

Since 2020, the population density of *L. brandtii* has remained high, necessitating large-scale rodent control measures during the spring and summer of 2023. These efforts resulted in a relatively low number of rodents collected that year. However, *L. brandtii* continues to dominate the rodent population and is expected to rebound, posing an ongoing threat as a primary vector of local rodent-borne diseases. Other rodent species, such as *Apodemus agrarius* and *Apodemus peninsulae*, are also present in the Hulunbuir area and may carry pathogens, such as *Yersinia pestis* and Hantaan virus (HTNV). Current research on *L. brandtii* focuses on its role in disrupting the ecological balance of grasslands and monitoring severe infectious diseases such as plague and hemorrhagic fever

with renal syndrome (HFRS). However, there is a lack of systematic studies on the unknown and potential pathogens that *L. brandtii* may harbour. Given the high infection rate of the Amugulang virus in this species, further research is needed to understand the risks of infection and transmission to predators, such as wolves, foxes, and weasels, and their impact on maintaining the local ecological balance.

The grasslands of Hulunbuir serve as traditional grazing areas for cattle and sheep, and *L. brandtii* is frequently found in grasslands, animal pens, and herder settlements. Notably, a significant abundance of *L. brandtii* has been observed in residential areas and near the sampling site in the Amugulang area. Their excrement and secretions can contaminate the environment and potentially human food sources. Although there is no definitive evidence linking *L. brandtii* to human infection, its genetic similarity to viruses, such as the Puumala virus (PUUV) and Muju virus, which can infect humans, raises concerns. Thus, the potential of *L. brandtii* to contribute to other febrile infectious diseases, particularly among vulnerable populations such as children and the elderly, warrants attention.

Hantavirus evolution in molecular epidemiology involves three main mechanisms: genomic mutations, reassortment of segmented genomes between closely related hantaviruses, and genetic recombination. Various members of the *Hantaviridae* family, such as HTNV and Seoul virus (SEOV), are prevalent in northern China, including the northern and eastern parts of Inner Mongolia. These viruses can spread through the inhalation and ingestion of secretions, excreta, or bites from infected parasites. As animals migrate, the virus spreads. The Hulunbuir region's extensive land border with Mongolia and Russia facilitates the seasonal migration of wild animals such as

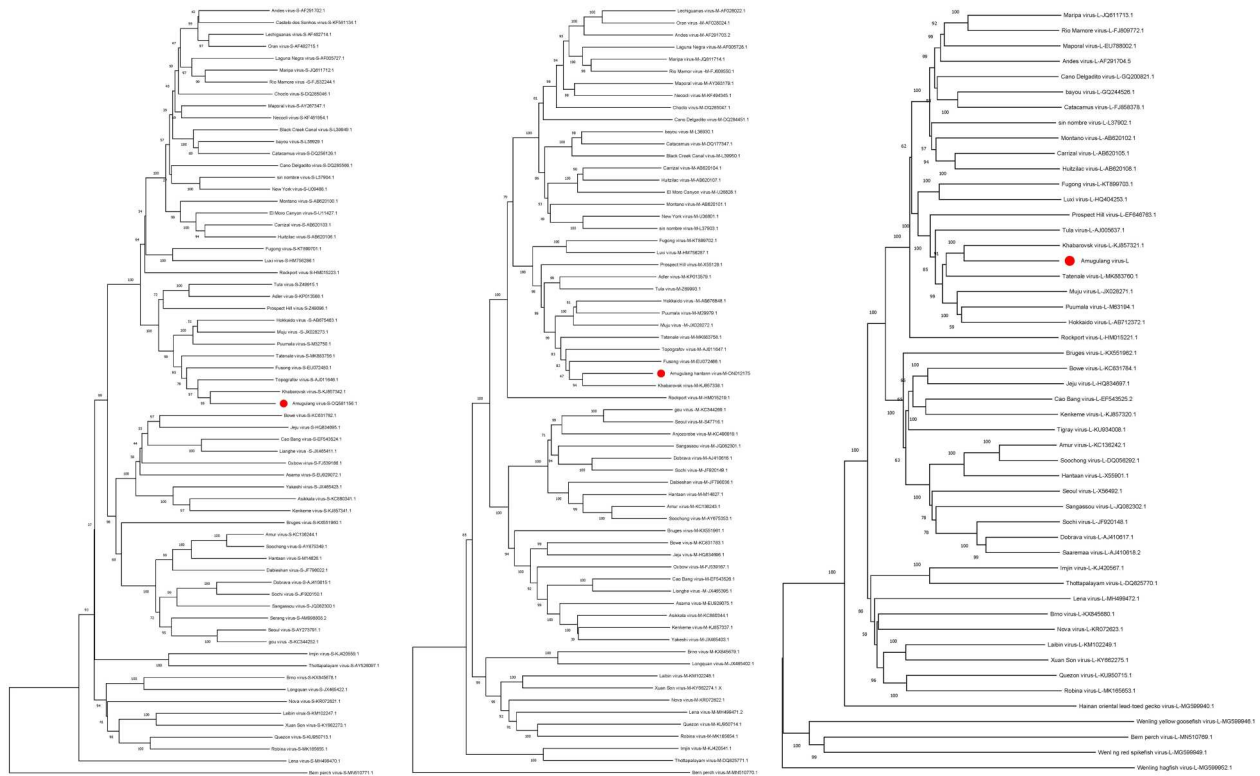


**Figure 5.** The NJ tree of the Amugulang virus S (left), M (middle), and L (right) segments.

Note: The system evolution parameters are as follows: 1. Constructed using Neighbour-Joining method; 2. Test of Phylogeny: Bootstrap method; 3. No. of Bootstrap Replications: 1000; 4. Gaps/Missing Data Treatment: Complete deletion.

yellow sheep, wolves, and foxes. Active wild rodents on both sides of the border enable long-distance transmission of viruses, leading to interactions between Amugulang virus and HTNV both domestically and internationally. Recombination of hantaviruses, such as PUUV, increases the risk of human infection.

Rodents are generally considered the primary natural hosts of hantaviruses, adhering to the “one-mammal-one-hantavirus rule” or “single-host-single-virus systems” [22]. In this study, attempts to infect BALB/c and Kunming mice with Amugulang virus via oral, nasal, or intraperitoneal routes were unsuccessful, and the virus was not detected in samples from other species in the region. This suggests that the Amugulang virus is highly adapted and co-evolved with *L. brandtii*, following the “one-mammal-one-hantavirus rule.” However, this rule is not absolute, as recent discoveries of various hantaviruses have revealed a broader range of hosts, including shrews, bats, freshwater fish, geckos, and lower vertebrates [3]. Although hantaviruses typically select a specific host with which they co-adapt and evolve, exceptions exist, such as SEOV, which infects at least two rodent species. Humans are considered a “dead end” in hantavirus evolution, with epidemics not contributing to virus evolution [24].

The relatively strict “single-host-single-virus systems” of hantaviruses make isolation challenging. Even when successfully infecting cells, virus growth

is slow and its titre remains low [25]. Previous attempts to isolate the Amugulang virus using conventional methods, such as inoculating Vero cells with organ homogenate from positive samples and conducting nucleic acid tests after three generations of blind passages, have been unsuccessful, as described in the literature. Vero cells, which are commonly used to isolate hantaviruses, have a low success rate. It is likely that the cells most suitable for isolating the Amugulang virus are primary cells of *L. brandtii*, which require long-term cultivation for successful isolation.

*Hantaviridae* are pleomorphic, with diameters ranging from 120–160 nm and variable shapes ranging from round to elongated. In this study, Amugulang virus particles exhibited a relatively regular shape, with diameters of 120–160 nm and spikes extending approximately 10 nm from the surface. The viral particles were observed at different cellular locations and displayed varying sizes and morphologies. It is generally believed that viral particles assemble in the Golgi apparatus, enter the Golgi pool through budding, and are released via exocytosis (Old World hantaviruses, distributed in Europe and Asia), transported to the cell surface, or directly released onto the plasma membrane (New World hantaviruses, distributed in North and South America) [16,23]. However, the details of this process remain unclear. In this study, virions located in Golgi vesicles appeared to be fully

**Table 3.** Genetic distances of nucleotide and amino acid sequences of the tandem sequence of the Amugulang virus S, M, L, and S-M segments.

Amugulang virus	Seg S		Seg M		Seg L		Seg S-M	
	aa	nt	aa	nt	aa	nt	aa	nt
Adler virus	17.991	24.961	19.947	—	—	—	19.334	27.325
Amur virus	36.066	36.456	45.053	43.383	30.279	33.282	42.342	41.180
Andes virus	27.336	30.327	32.865	38.345	21.897	28.920	31.074	34.976
Anjzorobe virus	40.930	38.581	45.841	44.558	—	—	—	—
Asama virus	—	—	47.401	46.322	—	—	45.356	43.859
Asikkala virus	40.376	41.484	46.208	43.598	—	—	44.409	42.923
Bayou virus	25.467	30.560	32.337	36.762	21.711	28.563	30.179	34.261
Bern perch virus	82.683	64.831	89.683	66.379	75.405	60.983	87.492	64.556
Black Creek Canal virus	25.234	29.860	32.601	36.611	—	—	30.243	33.772
Bowe virus	38.498	38.486	46.561	43.509	33.628	34.430	44.116	42.057
Brno virus	47.518	42.484	58.090	50.407	37.962	35.500	55.110	47.700
Bruges virus	41.121	39.019	46.032	44.270	31.349	33.919	44.544	42.774
Cano Delgadito virus	28.505	30.016	34.007	38.679	21.339	28.263	32.417	35.699
Cao Bang virus	38.967	38.407	46.296	45.071	29.767	32.413	43.987	42.457
Carrizal virus	27.103	31.260	31.168	34.945	21.292	28.159	29.904	33.700
Castelo dos Sonhos virus	28.912	33.552	—	—	—	—	—	—
Catacamus virus	25.935	31.260	32.513	37.216	21.804	28.666	30.499	34.445
Choclo virus	26.636	30.949	34.446	38.225	—	—	32.097	35.282
Dabieshanense virus	36.534	34.348	44.867	46.398	—	—	42.370	41.948
Dobrava virus	37.705	37.315	45.318	45.376	30.326	33.750	43.050	42.747
El Moro Canyon virus	27.570	31.104	32.221	34.844	—	—	30.735	33.486
Fugong virus	24.826	28.538	27.441	30.700	20.502	27.602	26.407	29.833
Fusong virus	9.513	19.751	12.379	23.654	—	—	11.438	22.192
Gou virus	36.534	35.831	44.779	44.916	—	—	42.332	41.979
Hainan oriental lead-toed gecko virus	—	—	—	—	47.922	43.535	—	—
Hantaan virus	35.831	37.627	44.788	43.843	30.558	33.590	42.085	41.979
Hokkaido virus	11.601	23.717	15.189	24.157	10.414	23.732	14.121	24.079
Huitzilac virus	27.336	31.960	31.343	35.801	21.339	29.116	30.032	34.495
Imjin virus	53.412	45.027	56.810	51.301	38.472	37.496	55.974	50.207
Jeju virus	41.080	39.032	45.944	44.095	32.512	34.305	44.437	42.351
Kenkeme virus	40.845	39.844	47.090	45.630	30.930	33.385	45.180	43.600
Khabarovsk virus	6.032	15.474	5.975	18.196	4.231	18.647	5.818	17.215
Laguna Negra virus	26.636	31.182	33.128	38.477	—	—	31.138	35.710
Laibin virus	46.370	41.810	53.072	47.299	34.967	35.336	50.973	45.356
Lechiguanas virus	27.336	30.793	32.777	38.326	—	—	31.074	35.362
Lena virus	52.941	47.105	53.778	51.552	38.293	38.264	53.562	49.676
Lianghe virus	38.732	37.939	48.413	45.274	—	—	45.466	42.642
Longquan virus	45.626	41.831	58.422	50.582	—	—	54.828	47.309
Luxi virus	25.290	28.305	27.001	30.750	20.419	28.191	26.215	30.046
Maporal virus	26.869	31.571	33.949	37.879	21.339	27.974	31.734	35.364
Maripa virus	26.869	30.793	32.337	36.762	21.525	28.931	30.563	34.455
Montano virus	26.402	30.560	33.450	35.786	21.711	28.798	31.374	34.047
Muju virus	12.529	21.773	13.345	24.056	11.111	23.255	13.035	23.196
Necocli virus	28.271	31.104	33.216	38.074	—	—	31.586	35.119
New York virus	27.336	31.260	32.397	36.606	—	—	30.863	34.454
Nova virus	47.196	42.980	53.695	48.904	38.064	36.936	51.427	46.712
Oran virus	27.570	30.793	32.865	39.637	—	—	31.138	36.097
Oxbow virus	40.000	39.515	46.737	43.191	—	—	44.695	42.269
Prospect Hill virus	17.401	23.950	21.705	30.363	15.628	26.106	20.205	27.823
Puumala virus	12.993	23.250	16.945	24.610	11.297	23.039	15.783	24.170
Quezon virus	42.857	38.768	54.756	50.868	36.444	37.862	51.197	45.696
Rio Mamor virus	27.103	30.638	32.425	37.166	21.478	28.920	30.691	34.517
Robina virus	44.028	40.827	53.125	50.901	36.800	37.926	50.130	47.004
Rockport virus	27.570	31.726	37.093	38.213	24.558	30.008	34.337	35.876
Saaremaa virus	—	—	—	—	30.512	33.811	—	—
Sangassou virus	37.002	36.768	45.936	44.785	30.326	33.647	43.308	41.777
Seoul virus	36.534	36.612	44.602	45.478	30.605	34.510	42.204	42.317
Serang virus	36.534	37.002	—	—	—	—	—	—
Sin nombre virus	27.570	30.404	31.607	37.009	20.828	28.611	30.415	34.393
Sochi virus	38.173	37.549	45.310	45.989	30.140	33.709	43.235	43.024
Soochong virus	36.534	35.597	45.141	43.383	30.326	33.976	42.535	40.719
Tatenale virus	11.833	22.240	12.680	24.409	9.995	21.887	12.354	23.623
Thottapalayam virus	52.594	45.341	56.043	51.221	38.128	37.883	55.036	50.048
Tigray virus	—	—	—	—	31.116	33.040	—	—
Topografov virus	4.640	17.729	8.963	21.976	—	—	7.673	20.384
Tula virus	17.799	24.299	18.190	27.680	13.767	24.684	18.054	26.581
Wenling hagfish virus	—	—	—	—	83.350	57.259	—	—
Wenling red spikefish virus	—	—	—	—	74.090	60.618	—	—
Wenling yellow goosfish virus	—	—	—	—	78.139	61.021	—	—
Xuan Son virus	44.731	40.796	52.004	47.418	34.407	35.446	49.665	45.486
Yakeshi virus	37.793	38.750	47.090	45.071	—	—	44.344	42.954



assembled, with free virus particles measuring 120–160 nm in diameter and visible capsules. Slender virions were not observed in this study. Additionally, no large clusters of viral particles were found within the cells, likely due to the high adaptation of the virus to its host cell. A slower proliferation rate may contribute to the persistent infections observed in host organisms.

## Conclusion

A novel member of the *Hantaviridae* family, the Amugulang virus, was identified in *L. brandtii* from Hulunbuir, China, with an infection rate of 7.5%. Viral particles were localized in the cytoplasm of renal cells, measuring 120–160 nm, with a capsule membrane. The virus was unable to infect and replicate in BALB/c or Kunming mice, Vero cells, or BHK-21 cells, and did not achieve vertical placental transmission. Antigenic cross-reactivity with HFRS virus was observed. Phylogenetic analysis indicated that the Amugulang virus is most closely related to the Khabarovsk virus isolated from the Russian Far East.

## Disclosure statement

No potential conflict of interest was reported by the author(s).

## Funding

This study was supported by the Science and Technology Partnership Program of the Ministry of Science and Technology of China (KY201901014) and the National Key R&D Program of China (2022YFC2303700).

## Additional information

### Ethical statement

The study was approved by Shenyang Agriculture University (Letter Number: 2021040701).

### Authors' contributions

Xiaohu Han and Zeliang Chen conceptualized the initial hypothesis, and conceived and designed the study. Feng Jiang, Xiaohu Han, Lianhong Zhang, Mei Han, Yongxiang Zhao, Ya Wen, Hua Deng, Feng Jiang, Mingxuan Zhang and Saijilahu performed the sample collection and molecular detection. Qin Dai, Jinguo Zhang and Lianhong Zhang collected sorted data. Qing Xin and Tianyu Yang, edited the tables. Xiaohu Han and Zeliang Chen conducted literature searches and participated in the writing process. Xiaohu Han, Lianhong Zhang performed the statistical analyses and wrote the first draft of the manuscript. Xiaohu Han and Zeliang Chen revised the manuscript. All authors contributed substantially to the data acquisition, interpretation, and revision and editing of the manuscript.

## References

- [1] Abudurexiti A, Adkins S, Alioto D, et al. Taxonomy of the order *Bunyavirales*: update 2019. *Arch Virol*. 2019;164(7):1949–1965. doi:10.1007/s00705-019-04253-6
- [2] Laenen L, Vergote V, Calisher CH, et al. *Hantaviridae*: current classification and future perspectives. *Viruses*. 2019;11(9):788. doi:10.3390/v11090788
- [3] Kuhn JH, Schmaljohn CS. A brief history of bunyaviral family *Hantaviridae*. *Diseases*. 2023;11(1):38. doi:10.3390/diseases11010038
- [4] Clement J, Maes P, Van Ranst M. Hemorrhagic fever with renal syndrome in the new, and Hantavirus pulmonary syndrome in the old world: paradisiacal lost or regained? *Virus Res*. 2014;187:55–58. doi:10.1016/j.virusres.2013.12.036
- [5] Avšič-Županc T, Saksida A, Korva M. Hantavirus infections. *Clin Microbiol Infect*. 2019;21:e6–e16. doi:10.1111/1469-0691.12291
- [6] Krüger DH, Ulrich R, Lundkvist Å. Hantavirus infections and their prevention. *Microbes Infect*. 2001 2001/11/01;3(13):1129–1144. doi:https://doi.org/10.1016/S1286-4579(01)01474-5.
- [7] Noh JY, Jung J, Song J-W. Hemorrhagic fever with renal syndrome. *Infect Chemother*. 2019;51(4):405–413. doi:10.3947/ic.2019.51.4.405
- [8] Brummer-Korvenkontio M, Vaheri A, Hovi T, et al. Nephropathia Epidemica: detection of antigen in bank voles and serologic diagnosis of human infection. *J Infect Dis*. 1980;141(2):131–134. doi:10.1093/infdis/141.2.131
- [9] Williams EP, Taylor MK, Demchyshyna I, et al. Prevalence of hantaviruses harbored by murid rodents in northwestern Ukraine and discovery of a novel puumala virus strain. *Viruses*. 2021;13(8):1640. doi:10.3390/v13081640
- [10] Alemán A, Iguarán H, Puerta H, et al. Hantaviruses: a global disease problem. *Emerg Infect Dis*. 1997;3(2):95–104. *Revista De Salud Pública*. 1997. doi:10.3201/eid0302.970202
- [11] Sanada T, Seto T, Ozaki Y, et al. Isolation of Hokkaido virus, genus Hantavirus, using a newly established cell line derived from the kidney of the grey red-backed vole (*Myodes rufocanus bedfordiae*). *J Gen Virol*. 2012;93(10):2237–2246. doi:10.1099/vir.0.045377-0
- [12] Hörling J, Chizhikov V, Lundkvist Å, et al. Khabarovsk virus- a phylogenetically and serologically distinct Hantavirus isolated from *Microtus fortis* trapped in far-east Russia. *J Gen Virol*. 1996;77(4):8. doi:10.1099/0022-1317-77-4-687
- [13] Ge X-Y, Yang W-H, Pan H, et al. Fugong virus, a novel hantavirus harbored by the small oriental vole (*Eothenomys eleusis*) in China. *Virol J*. 2016;13(1):27. doi:10.1186/s12985-016-0483-9
- [14] Chappell JG, Tsoleridis T, Onianwa O, et al. Retrieval of the complete coding sequence of the UK-Endemic Tatenale *Orthohantavirus* reveals extensive strain variation and supports its classification as a novel species. *Viruses*. 2020;12(4):454. doi:10.3390/v12040454
- [15] Meheretu Y, Stanley WT, Craig EW, et al. Tigray *Orthohantavirus* infects two related rodent species adapted to different elevations in Ethiopia. *Vector-Borne Zoonotic Diseases*. 2019;19(12):950–953. doi:10.1089/vbz.2019.2452
- [16] Meier K, Thorkelsson SR, Quemin ERJ, et al. Hantavirus replication cycle—An updated structural

- virology perspective. *Viruses*. 2021;13(8):1561. doi:10.3390/v13081561
- [17] Plyusnin A, Vapalahti O, Vaheri A. Hantaviruses: genome structure, expression and evolution. *J Gen Virol*. 1996 Nov;77(Pt 11):2677–2687. PubMed PMID: 8922460; eng. doi:10.1099/0022-1317-77-11-2677
- [18] Maes P, Klempa B, Clement J, et al. A proposal for new criteria for the classification of hantaviruses, based on S and M segment protein sequences. *Infect Genet Evol*. 2009 2009/09/01;9(5):813–820. doi:https://doi.org/10.1016/j.meegid.2009.04.012.
- [19] Taki Y, Vincenot CE, Sato Y, et al. Genetic diversity and population structure in the Ryukyu flying fox inferred from remote sampling in the Yaeyama archipelago. *PLoS One*. 2021;16(3):e0248672. doi:10.1371/journal.pone.0248672
- [20] Song KJ, Baek LJ, Moon S, et al. Muju virus, a novel hantavirus harboured by the arvicolid rodent *Myodes regulus* in Korea. *J Gen Virol*. 2007 Nov;88(Pt 11):3121–3129. PubMed PMID: 17947538; PubMed Central PMCID: PMC2253664. eng. doi:10.1099/vir.0.83139-0
- [21] Parvate A, Williams EP, Taylor MK, et al. Diverse morphology and structural features of old and new world hantaviruses. *Viruses*. 2019;11(9):862. doi:10.3390/v11090862
- [22] Mull N, Jackson R, Sironen T, et al. Ecology of neglected rodent-borne American *Orthohantaviruses*. *Pathogens*. 2020;9(5):325. doi:10.3390/pathogens9050325
- [23] Battisti AJ, Chu Y-K, Chipman PR, et al. Structural studies of hantaan virus. *J Virol*. 2011;85(2):835–841. doi:10.1128/jvi.01847-10
- [24] Plyusnin A, Morzunov SP. Virus evolution and genetic diversity of hantaviruses and their rodent hosts. In: Schmaljohn CS, Nichol ST, editors. *Hantaviruses*. Berlin, Heidelberg: Springer Berlin Heidelberg; 2001. p. 47–75.
- [25] Meyer BJ, Schmaljohn C. Accumulation of terminally deleted RNAs may play a role in Seoul virus persistence. *J Virol*. 2000 Feb;74(3):1321–1331. PubMed PMID: 10627543; PubMed Central PMCID: PMC111467. eng. doi:10.1128/jvi.74.3.1321-1331.2000